The Journal of Engineering

The 7th International Conference on Renewable Power Generation (RPG 2018)

IET Journals
The Institution of Engineering and Technology

Modifying the control design of DFIG-based wind turbines in order to inhibit power system oscillations

eISSN 2051-3305
Received on 26th October 2018
Accepted on 10th January 2019
E-First on 28th June 2019
doi: 10.1049/joe.2018.9260
www.ietdl.org

Mohammad Jafarian[1] ✉, *Mohammad-Naser Asefi*[1]

[1]*Power System Studies Group, Niroo Research Institute, Tehran, Iran*

✉ *E-mail: mjafarian@nri.ac.ir*

Abstract: Providing additional damping for system electromechanical oscillations through doubly fed induction generator (DFIG)-based wind turbines is investigated in this study. In this regard, first an objective function is developed to tune the DFIG control gains, aim to maximise the wind farm (WF) contribution to system oscillation damping, but it is shown that it causes a decrease in the damping of DFIG stator mode. In other words, with the current DFIG control design, it is not possible to improve both the small signal stability of the power system and the dynamic stability of WF together. Afterwards, two high-pass filters are suggested to be employed in the control design of DFIG. It is shown that with the modified control design, it is possible to improve the system oscillation without spoiling the dynamic stability of the WF itself. Eigenvalue analysis is performed to validate the effectiveness of the modified control design.

1 Introduction

Small signal stability is the ability of a power system to maintain synchronism when subjected to small disturbances. In today's power systems, the small signal stability problem is usually the lack of sufficient damping torque for system electromechanical oscillations [1]. Traditionally, the small signal stability of power systems is determined by the interactions of system synchronous generators (SGs) [2], but with the integration of large amounts of new wind generation, they can contribute to oscillation damping and affect the small signal stability of system [3].

Variable speed wind turbines utilising doubly fed induction generator (DFIG) are currently the most popular scheme in wind conversion systems [4]. Several research efforts have been devoted to studying the impact of DFIG-based wind farms (WFs) on the small signal stability of power systems. In [5], it is shown that DFIGs have detrimental interaction with some of the system oscillations and they may cause instability in some scenarios.

Considering the probable detrimental interactions, several research efforts have focused on the idea of providing additional damping for system oscillations through DFIG-based wind turbines. To do that, in most of these studies a supplementary control loop, referred to as wind power system stabiliser (WPSS), have been proposed in the control structure of wind turbine. The WPSS typically consists of a washout filter, a proportional controller, and a lead/lag block, as depicted in Fig. 1 [6].

The output signal of WPSS is added to the wind turbine pitch control, active power control, or reactive power/voltage control loops [6].

In [5], the grid frequency is selected as the input to WPSS and the WPSS output is added to the active power control loop. In [7, 8], the relative rotor angle difference of two system SGs is selected as the input and the output is added to the active power and reactive power control loops, respectively. In [9], a combination of remote and locally available signals is used as the WPSS input. In [3], locally available signals are selected for the input and the output is added to the active power control loop.

Fig. 1 *Typical WPSS*

To use remote signals as the WPSS input, the power system should have equipped with measurement systems (such as phasor measurement units). In this paper, it is shown that without WPSS or any new control loops, and with only some modifications in the control design of DFIGs, it is possible to provide additional damping for system oscillations, while holding the dynamic performance of WF unchanged.

2 Modelling the DFIG-based WFs

For power system studies, where we are interested in the probable impact of WF dynamics on transmission network, it is common to group the wind turbines and lump the whole farm into a single aggregated model [10, 11]. A DFIG-based wind turbine consists of the turbine, generator, drive train, and converter. The models used to describe the dynamics of the turbine, drive train, and generator are expressed in detail in [12]. The wind turbine converter is composed of three parts: grid-side converter; DC link, and rotor-side converter. If switching frequency is high enough and the switching loss is ignored, for power system stability studies it is possible to neglect the dynamics related to the grid-side converter and DC link [7].

To model the rotor-side converter, a decoupling control strategy, which enables decoupled control of DFIG's active and reactive powers, is used. This control strategy was developed in [13] and since then it has been frequently used in power system study researches [14–16]. It can be shown that the q-axis and d-axis rotor currents (i_{qr} and i_{dr}) can independently control the DFIG active and reactive powers, respectively [7]. The rotor currents themselves can be regulated by the injected q-axis and d-axis rotor voltages (u_{qr} and u_{dr}), respectively. This control strategy is presented in Fig. 2. Fig. 2 also depicts the suggested high-pass filters (shown with dashed lines), which are not involved originally in the control design of DFIGs, but (as will be discussed in Section 5) they can provide additional damping for system oscillation.

3 Impact of WF dynamics on network oscillation damping

To evaluate the impact of WF dynamics on network oscillation damping, a test system was developed in which a 1000 mega volt ampere (MVA) SG transmits 650 MW to a strong system (represented as an infinite bus) and also supplies a 150 MW local load (represented as constant impedance). Also, a 300 MW DFIG-

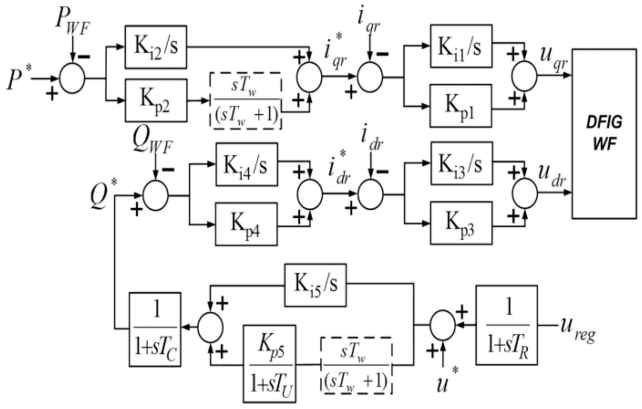

Fig. 2 *DFIG rotor-side converter control block diagram*

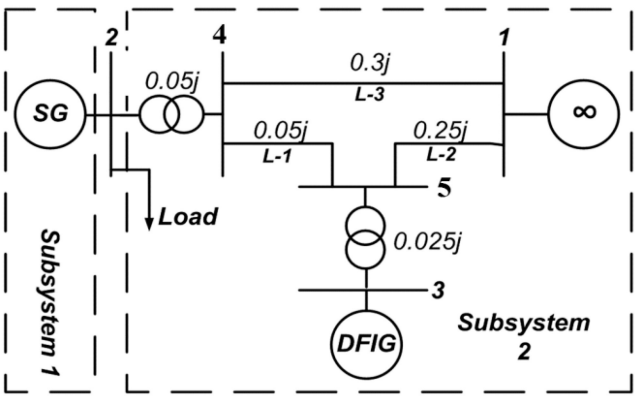

Fig. 3 *Test system*

based WF is connected near the SG on the high-voltage system via a step-up transformer. Fig. 3 depicts the one-line diagram of the test system. In this figure, impedances are presented in per unit on the MVA base of the SG.

Recently in [12], a new approach has been developed to investigate the impact of WF dynamics on system oscillation damping. In this approach, the test system is divided into two separate subsystems: Subsystem 1 which contains the system SGs and Subsystem 2 which contains the WF and transmission network.

When there is no WF in the system, Subsystem 2 can be described using the transmission network Jacobian matrix as

$$[\Delta p_2 \Delta q_2]^{\mathrm{T}} = \boldsymbol{J}[\Delta\theta_2 \Delta u_2]^{\mathrm{T}} \tag{1}$$

where Δp_2 and Δq_2 are the incremental changes in the active and reactive powers injected into bus 2, respectively, $\Delta\theta_2$ and Δu_2 are the incremental changes in the bus 2 voltage phase and magnitude, respectively, and $\boldsymbol{J}$ is the transmission network Jacobian matrix that can be expressed as

$$\boldsymbol{J} = \begin{bmatrix} J_{\mathrm{p}\theta} & J_{\mathrm{p}u} \\ J_{q\theta} & J_{qu} \end{bmatrix} \tag{2}$$

where $J_{\mathrm{p}\theta}$, $J_{\mathrm{p}u}$, $J_{q\theta}$, and $J_{qu}$are its elements (the details can be found in [12]).

When the WF is integrated into the system, the dynamics of Subsystem 2 can be described in the form of the transfer function as

$$[\Delta p_2 \Delta q_2]^{\mathrm{T}} = G[\Delta\theta_2 \Delta u_2]^{\mathrm{T}}$$
$$G = \begin{bmatrix} G_{\mathrm{p}\theta} & G_{\mathrm{p}u} \\ G_{q\theta} & G_{qu} \end{bmatrix} \tag{3}$$

where G is the transfer function of Subsystem 2 and $G_{\mathrm{p}\theta}$, $G_{\mathrm{p}u}$, $G_{q\theta}$, and G_{qu} are its elements (the details can be found in [12]). In [12], it is shown that an incremental change in the phase of $G_{\mathrm{p}\theta}$ considerably increases the damping of SG electromechanical mode, but variations in the other elements of this matrix negligibly affect the eigenvalue of this mode. Therefore, the phase of $G_{\mathrm{p}\theta}$ can be considered as an index to evaluate the impact of WF dynamics on network oscillation damping, so that if with the integration of WF into the system the phase of $G_{\mathrm{p}\theta}$ increases (decreases), the damping of system oscillation improves (gets worst).

4 Optimal tuning of DFIG control gains

DFIG-based wind turbines have three different operating modes: sub-synchronous speed, synchronous speed, and super-synchronous speed. To have a robust control, it is necessary to investigate the stability of WF in all these operating modes [17]. Also, as mentioned in Section 2, DFIGs have three control loops: active power, voltage, and pitch control loops. Therefore, to have a robust and optimal control, it is unavoidable to use optimisation algorithms to tune the DFIG control gains. In this regard, a genetic algorithm is used in [18] to improve the transient responses of DFIG rotor current and DFIG terminal voltage. Differential evolution and PSO algorithms are used in [4, 19], respectively, aim to shift all the WF eigenvalues as far to the left-hand side of the *S*-plane. In [20], bacterial foraging optimisation algorithm is used to increase the damping ratio of WF modes. To reduce the DFIG rotor overcurrent, the PSO algorithm is used in [21].

With the developed index, it is possible to tune the DFIG control gains aim to maximise the system oscillation damping. In this regard, two-objective functions are defined in this section: objective function A in which only the small signal stability of WF is taken into account and objective function B in which beside the stability of WF itself, enhancement of system oscillation damping is considered too. These objective functions are used to tune the DFIG control gains.

4.1 Objective function A

In the literature to investigate the stability of WFs, two criteria are taken into account: the lowest damping of WF modes and the lowest damping ratio of WF modes. In this paper, three different wind speeds are considered: 9, 12, and 19 m/s, which belong to sub-synchronous speed, synchronous speed, and super-synchronous speed operating modes, respectively. The lowest damping of WF modes in all the three considered operating points (O_1) can be expressed as

$$O_1 = \min(\sigma_{ik}), \quad i = 1, 2, 3 \tag{4}$$

where $\sigma_{ik}$is the damping of the kth WF mode in the ith considered the operating point. The lowest damping ratio of WF modes in all the three considered operating points *(O_2)* can be expressed as

$$O_2 = \min(\xi_{ik}), \quad i = 1, 2, 3 \tag{5}$$

where $\xi_{ik}$is the damping ratio of the kth WF mode in the ith considered the operating point.

As it was discussed, to enhance the small signal stability of WF, O_1 and O_2 should be maximised at the same time. The results of modal analysis technique show that the DFIG stator mode has the lowest damping ratio value and the mode related to the DFIG pitch control loop has the lowest damping value in all the three considered operating points (details are presented as follows). Therefore, there is no trade-off between increasing the stability margin and the damping ratio of WF modes and the weighted-sum method [18] can be used to handle this two-objective optimisation problem. In this regard objective function A is written as the weighted sum of O_1 and O_2 as

$$\text{maximum:} \quad \mathrm{Obj_A} = a_1 O_1 + a_2 O_2 \tag{6}$$

where a_1 and a_2 are the weighting factors (selected heuristically equal to 0.23 and 0.77, respectively). The optimum solution is not sensitive to the selections of a_1 and a_2.

4.2 Objective function B

As discussed before, in order to maximise the system oscillation damping through WF, the phase of $G_{P\theta}$ in the frequency of system oscillation (1.65 Hz) should be maximised. Since the frequency of system oscillation may change with the change of system operating conditions, we also considered two other frequencies in the vicinity of 1.65 Hz (1.48 and 1.80 Hz). In this regard, O_3 is defined as the weighted sum of the phase of $G_{p\theta}$ in 1.48, 1.65, and 1.8 Hz at the three considered WF operating points as

$$O_3 = \sum_{i=1}^{3} c_i \left(\sum_{m=1}^{3} d_m (\angle G_{p\theta,\, i}(j2\pi f_m)) \right) \tag{7}$$

where $c_i$is the weighting factor for the ith operation point; $f_m$and d_m are the mth considered frequency and its corresponding weighting factor, respectively, and $\angle G_{p\theta,\, i}(j2\pi f_m)$ is the phase of $G_{p\theta}$ in the mth considered frequency at the ith considered WF operating point. To maximise the system oscillation damping through WF, O_3 should be maximised.

In objective function B, the aim is to improve both the small signal stability of WF and the system oscillation damping. Therefore, the objectives O_1, O_2, and O_3 should be maximised together. It was noted that maximising O_2 is in conflict with maximising O_3 (details are presented as follows) which suggests that there is a trade-off between increasing the minimum damping ratio of WF modes and increasing the phase of $G_{p\theta}$ in 1.65 Hz (increasing the damping of system oscillation). Hence, the weighted-sum method is not useful alone in this case.

To solve this problem, the ε-constraint method is used together with the weighted-sum method. Since PSO algorithm is developed originally for non-linear optimisation problems with continuous variables, we used this method to optimise the proposed objective functions and search for the optimal DFIG control gains (which are presented in Table 1).

Table 2 shows the WF modes which have the lowest damping ratio in each of the considered operating points. By performing modal analysis, it was noted that the DFIG stator fluxes (ψ_{qs} and ψ_{ds}) have the highest participation factors in these modes. Considering the results of Table 2, it can be said that by using objective function B, the damping ratio values of DFIG stator mode has considerably decreased. Therefore, it can be concluded that with the current DFIG control design, providing additional damping for system oscillation through WF will cost considerable reduction in the damping ratio of DFIG stator mode.

5 Modifying the DFIG control design

Considering the results of Table 1, it can be said that the major difference between the DFIG control gains obtained using objective function A and objective function B is that K_{p2} and K_{p5} are almost zero in the latter case. It means that with the decrease in K_{p2} and K_{p5}, the phase of $G_{p\theta}$ is 1.65 Hz (and hence the system oscillation damping) increases, but the damping of DFIG stator mode decreases. To investigate this idea, we decreased the values of K_{p2} and K_{p5} from their original values (obtained using objective function A) to 10% of their original values (in steps of 15%). Fig. 4 shows the phase of $G_{p\theta}$ in these cases. As it can be seen, with the decrease in K_{p2} and K_{p5}, the phase of $G_{p\theta}$ for frequencies between 0.5 and 2.2 Hz increases at synchronous speed and super-synchronous speed operating modes, while at sub-synchronous speed it nearly remains still. Fig. 5 shows the trajectory of DFIG stator mode with the decrease in K_{p2} and K_{p5}. It can be seen that with the decrease in K_{p2} and K_{p5}, the damping of DFIG stator mode remarkably decreases at all the operating modes. It was also noted that the damping values of other DFIG modes negligibly change with the decrease in K_{p2} and K_{p5} (details have not been presented here for the sake of limited space).

As it was shown, decreasing K_{p2} and K_{p5} has beneficial impact on system oscillations and detrimental impact on DFIG stator mode, but since the frequency of DFIG stator mode is much higher

Table 1 Optimal DFIG control gains

	Controller gain	With objective function A	With objective function B
active power control loop	K_{p1}	0.026	0.028
	K_{i1}	0.071	0.075
	K_{p2}	3.387	0.137
	K_{i2}	34.63	11.32
reactive power control loop	K_{p3}	0.017	0.048
	K_{i3}	8.606	7.707
	K_{p4}	7.358	2.320
	K_{i4}	12.30	11.74
voltage control loop	K_{p5}	19.42	0.231
	K_{i5}	69.00	69.83
pitch control loop	K_{p6}	1564	1546
	K_{i6}	1710	1719

Table 2 WF modes with the lowest damping ratio values

Operating mode (wind speed)	With objective function A			With objective function B			With high-pass filters		
	Damping	Frequency, Hz	Damping ratio, %	Damping	Frequency, Hz	Damping ratio, %	Damping	Frequency, Hz	Damping ratio, %
sub-synchronous speed	54	55.8	15.22	34	65.4	8.43	54	55.9	15.19
synchronous speed	78	67.3	18.22	31	67.5	7.28	78	67.2	18.2
super-synchronous speed	66	68.4	15.23	27	68.8	6.33	66	68.3	15.26

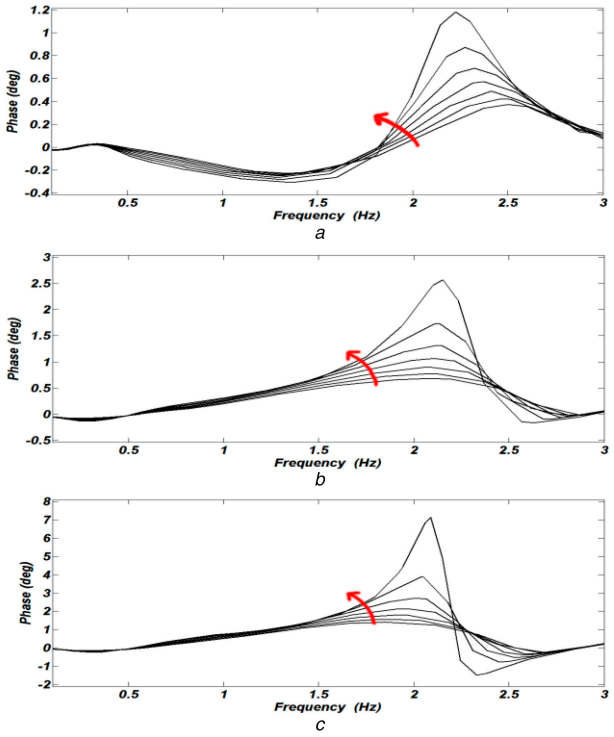

Fig. 4 *Phase of $G_{p\theta}$ at*

(a) Sub-synchronous speed, ***(b)*** Synchronous speed, ***(c)*** Super-synchronous speed operating modes (the arrows show the decrease in K_{p2} and K_{p5})

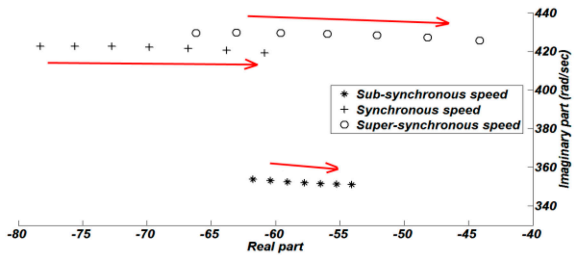

Fig. 5 *Eigenvalue of DFIG stator mode (the arrows show the decrease in K_{p2} and K_{p5})*

(about 60 Hz) than the frequency of system oscillation (about 1.65 Hz), they can be distinguished by using two high-pass filters in series with K_{p2} and K_{p5}, as depicted in Fig. 2. In this figure, the high-pass filters are shown with dashed lines. These filters attenuate the values of K_{p2} and K_{p5} for low-frequency signals (such as system oscillation) while passing high-frequency signals (such as DFIG stator mode).

The simplest high-pass filter is the first-order high-pass filter, known as washout filter. In this paper, we used the washout filter and, as it will be shown, it totally satisfies our goals. Using higher-order high-pass filters will cause higher time delays, and therefore increases the risk of spoiling the dynamic performance of WF. The transfer function of a washout filter can be expressed as

$$\mathrm{TF}_{\mathrm{washout}} = \frac{sT_{\mathrm{w}}}{1 + sT_{\mathrm{w}}} \tag{8}$$

where $\mathrm{TF}_{\mathrm{washout}}$ and T_{w} are the transfer function and the time constant of the washout filter and s is the Laplace parameter. After applying the washout filters in the DFIG control design, to study the impact of T_{w} on the damping provided for system oscillation through WF, we evaluated the phase of $G_{p\theta}$ for four different values of T_{w} (0.01, 0.07, 0.3, and 1 s). Fig. 6 shows the results. It can be said that high values of T_{w} (such as 0.3 and 1 s) insufficiently increase the phase of $G_{p\theta}$ at 1.65 Hz. Also, very low values of T_{w} (such as 0.01 s) decrease the phase of $G_{p\theta}$ in 1.65 Hz

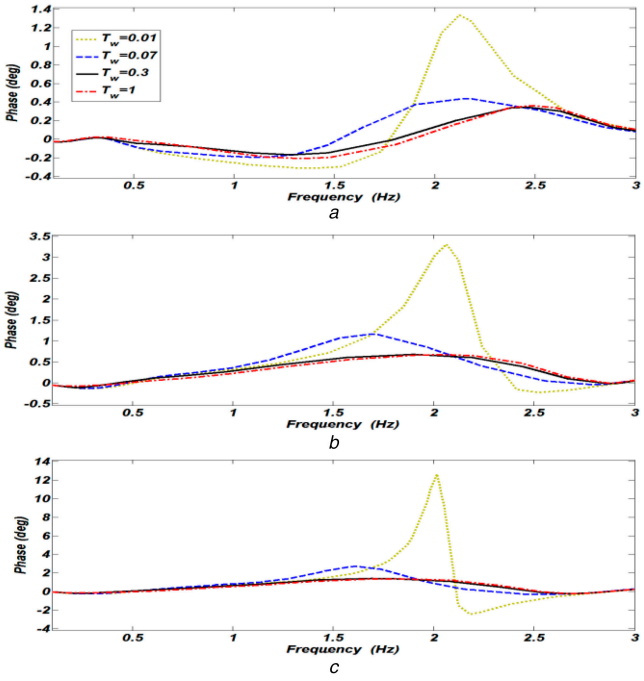

Fig. 6 *Phase of $G_{p\theta}$ for different values of T_w at*

(a) Sub-synchronous speed, ***(b)*** Synchronous speed, ***(c)*** Super-synchronous speed operating modes

at sub-synchronous speed operating mode. With moderate values of T_{w} (such as 0.07 s), the phase of $G_{p\theta}$ is positive for all the three WF operating modes. To select the optimum value of T_{w}, we repeated the PSO algorithm to optimise objective function B, but this time with T_{w} as the optimisation parameter. The optimum value was found to be 0.07 s.

Tables 2 and 3 show the lowest damping ratio values and the DFIG modes with the lowest damping values, respectively, when the washout filters are applied. Comparing the results, it can be said that by applying the washout filters, the WF dynamic performance has remained the same (as what it was with objective function A). Table 4 shows the frequency and damping of system oscillation. It can be said that with the washout filters, the damping values of system oscillation have improved at all the WF operating modes (compared with the ones with objective function A). Considering the results of Tables 2–4 together, it can be concluded that by applying the washout filters, the damping of system oscillation improves while the WF stability remains unchanged.

6 Conclusions

In this paper, providing additional damping for system electromechanical oscillations through DFIG-based WFs was investigated. To do that, two-objective functions were developed: one to maximise the dynamic stability of WF and the other to maximise both the system oscillation damping and the WF dynamic stability. These objective functions were used to tune the DFIG control gains and PSO algorithm was used as the optimisation algorithm. It was noted that using the latter objective function will result in the reduction of the damping of DFIG stator mode. In other words, with the current DFIG control design, it is not possible to improve both the small stability of the power system and the dynamic stability of WF itself.

It was noted that the main difference between the optimal gains obtained using the proposed objective functions is that the proportional gains of DFIG active power and DFIG voltage control loops vanish in the latter case. Since the frequency of DFIG stator mode is much higher than the frequency of system oscillation, they can be distinguished by employing two high-pass filters in series with these gains. These filters attenuate these gains for low-frequency signals (such as system oscillations) while passing high-frequency signals (such as DFIG stator mode). In this paper, the simplest high-pass filter, known as washout filter, was used. The

Table 3 WF modes with the lowest damping values

Operating mode (wind speed)	With objective function A			With objective function B			With high-pass filters		
	Damping	Frequency, Hz	Damping ratio, %	Damping	Frequency, Hz	Damping ratio, %	Damping	Frequency, Hz	Damping ratio, %
sub-synchronous speed	1.13	0.42	39.14	1.06	0.43	36.37	1.06	0.43	36.37
synchronous speed	1.23	0	100	1.23	0	100	1.25	0	100
super-synchronous speed	1.15	0	100	1.16	0	100	1.15	0	100

Table 4 Frequency and damping of system oscillation

Operating mode (wind speed)	With objective function A			With objective function B			With high-pass filters		
	Damping	Frequency, Hz	Damping ratio, %	Damping	Frequency, Hz	Damping ratio, %	Damping	Frequency, Hz	Damping ratio %
sub-synchronous speed	0.118	1.65	1.139	0.161	1.65	1.554	0.130	1.65	1.254
synchronous speed	0.137	1.65	1.321	0.175	1.65	1.685	0.157	1.65	1.511
super-synchronous speed	0.161	1.65	1.557	0.178	1.68	1.688	0.201	1.65	1.977

results of eigenvalue analysis showed that with applying the washout filters, the damping of system oscillation improves, while the stability of WF remains unchanged.

7 References

[1] Kundur, P.: '*Power system stability and control*' (McGraw-Hill, New York, 1994)

[2] Mei, F., Pal, B.: 'Modal analysis of grid-connected doubly fed induction generators', *IEEE Trans. Energy Convers.*, 2007, **22**, (3), pp. 728–736

[3] Tsourakis, G., Nomikos, B.M., Vournas, C.D.: 'Contribution of doubly fed wind generators to oscillation damping', *IEEE Trans. Energy Convers.*, 2009, **24**, (3), pp. 783–791

[4] Yang, L., Yang, G.Y., Xu, Z.*, et al.*: 'Optimal controller design of a doubly-fed induction generator wind turbine system for small signal stability enhancement', *IET Gener. Transm. Distrib.*, 2010, **4**, (5), pp. 579–597

[5] Gautam, D., Vittal, V., Harbour, T.: 'Impact of increased penetration of DFIG-based wind turbine generators on transient and small signal stability of power systems', *IEEE Trans. Power Syst.*, 2009, **24**, (3), pp. 1426–1434

[6] Domínguez-García, J.L., Gomis-Bellmunt, O., Bianchi, F.D.*, et al.*: 'Power oscillation damping supported by wind power: a review', *Renew. Sustain. Energy Rev.*, 2012, **16**, (7), pp. 4994–5006

[7] Miao, Z., Fan, L.: 'The art of modeling and simulation of induction generator in wind generation applications using high-order model', *Simul. Pract. Theory*, 2008, **16**, (9), pp. 1239–1253

[8] Fan, L., Yin, H., Miao, Z.: 'On active/reactive power modulation of DFIG-based wind generation for interarea oscillation damping', *IEEE Trans. Energy Convers.*, 2011, **26**, (2), pp. 513–521

[9] Hughes, F.M., Anaya-Lara, O., Jenkis, N.*, et al.*: 'Control of DFIG-based wind generation for power network support', *IEEE Trans. Power Syst.*, 2005, **20**, (4), pp. 1958–1966

[10] Bianchi, F.D., Battista, H.D., Mantz, R.J.: '*Wind turbine control systems: principles, modelling and gain scheduling design*' (Springer, London, 2007)

[11] Fernandez, R.D., Jurado, F., Saenz, J.R.: 'Aggregated dynamic model for wind farms with doubly fed induction generator wind turbines', *Renew. Energy*, 2008, **33**, (1), pp. 129–140

[12] Jafarian, M., Ranjbar, A.M.: 'Interaction of the dynamics of doubly fed wind generators with power system electromechanical oscillations', *IET Renew. Power Gener.*, 2013, **7**, (2), pp. 89–97

[13] Xu, L., Wei, C.: 'Torque and reactive power control of a doubly fed induction machine by position sensorless scheme', *IEEE Trans. Ind. Appl.*, 1995, **31**, (3), pp. 636–642

[14] Mendonca, A., Lopes, J.A.P.: 'Robust tuning of power system stabilisers to install in wind energy conversion systems', *IET Renew. Power Gener.*, 2009, **3**, (4), pp. 465–475

[15] Fan, L., Kavasseri, R., Miao, Z.L.*, et al.*: 'Modeling of DFIG-based wind farms for SSR analysis', *IEEE Trans. Power Deliv.*, 2010, **25**, (4), pp. 2073–2082

[16] Miao, Z., Fan, L., Osborn, D.*, et al.*: 'Control of DFIG-based wind generation to improve interarea oscillation damping', *IEEE Trans. Energy Convers.*, 2009, **24**, (2), pp. 415–422

[17] Mishra, Y., Mishra, S., Fangxing, L.*, et al.*: 'Small-signal stability analysis of a DFIG-based wind power system under different modes of operation', *IEEE Trans. Energy Convers.*, 2009, **24**, (4), pp. 972–982

[18] Vieira, J.P.A., Nunes, M.V.A., Bezerra, U.H.*, et al.*: 'Designing optimal controllers for doubly fed induction generators using a genetic algorithm', *IET Gener. Transm. Distrib.*, 2009, **3**, (5), pp. 472–484

[19] Wu, F., Zhang, X.P., Godfrey, K.*, et al.*: 'Small signal stability analysis and optimal control of a wind turbine with doubly fed induction generator', *IET Gener. Transm. Distrib.*, 2007, **1**, (5), pp. 751–760

[20] Mishra, Y., Mishra, S., Tripathy, M.*, et al.*: 'Improving stability of a DFIG-based wind power system with tuned damping controller', *IEEE Trans. Energy Convers.*, 2009, **24**, (3), pp. 650–660

[21] Qiao, W., Venayagamoorthy, G.K., Harley, R.G.: 'Design of optimal PI controllers for doubly fed induction generators driven by wind turbines using particle swarm optimization'. Int. Joint Conf. Neural Networks, Canada, 2006, pp. 1982–1987